Accepted Manuscript

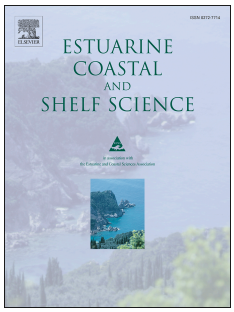

Thermal response to the surface heat flux in a macrotidal coastal region (Nuevo Gulf, Argentina)

Andrés L. Rivas, Juan P. Pisoni, Fernando G. Dellatorre

PII: S0272-7714(16)30126-3

DOI: 10.1016/j.ecss.2016.04.015

Reference: YECSS 5108

To appear in: *Estuarine, Coastal and Shelf Science*

Received Date: 9 November 2015

Revised Date: 20 April 2016

Accepted Date: 22 April 2016

Please cite this article as: Rivas, A.L., Pisoni, J.P., Dellatorre, F.G., Thermal response to the surface heat flux in a macrotidal coastal region (Nuevo Gulf, Argentina), *Estuarine, Coastal and Shelf Science* (2016), doi: 10.1016/j.ecss.2016.04.015.

TITLE

Thermal response to the surface heat flux in a macrotidal coastal region (Nuevo Gulf, Argentina)

AUTHORS AND AFFILIATIONS

Andrés L. Rivas*[(1,2)], Juan P. Pisoni[(1)] and Fernando G. Dellatorre[(1,2,3)]

[1] Centro para el Estudio de Sistemas Marinos (CESIMAR), CONICET, Bvd. Brown 2915 (U9120ACF), Puerto Madryn, Argentina.

[2] Universidad Nacional de la Patagonia, Sede Pto. Madryn. Bvd. Brown 3150, Puerto Madryn, Argentina.

[3] Universidad Tecnológica Nacional, Facultad Regional Chubut. Av. del Trabajo 1536 (9120). Puerto Madryn, Argentina.

*Corresponding author (ALR) Centro Nacional Patagónico (Consejo Nacional de Investigaciones Científicas y Técnicas de Argentina) – Bvd. Brown 2915 (U9120ACF), Puerto Madryn, Argentina Tel: +54-280-4883184 (Int 1241) E-mail: andres@cenpat-conicet.gob.ar

HIGHLIGHTS

- Surface heat flux and cross-shore advection modulate nearshore seasonal temperature fluctuations.
- Tidal height is very important in the regulation of nearshore daily temperature fluctuations.
- In summer, daily temperature anomaly reaches 4°C during low tide.

ABSTRACT

At mid-latitudes, sea water temperature shows a strong seasonal cycle forced by the incident surface heat flux. As depth decreases, the heat flux incidence is damped by the horizontal flux, which prevents the indefinite growth of the seasonal temperature range. In the present work, cross-shore transport in the west coast of Nuevo Gulf (Argentina) was analyzed. Processes tending to cool the coastal waters in summer and to warm the coastal waters in winter, were identified through temperature measurements, surface heat flux and tidal height. The simplified models proposed here provide a feedback mechanism that links changes in surface heat flux with changes in the horizontal heat flux during both seasons. On shorter time scales, tide produces significant variations in the height of the water column, therefore influencing temperature fluctuations and the direction of the horizontal flow.

KEYWORDS

cross-shore exchange

diurnal temperature variability

tidal cycle

seasonal cycle

41 1. INTRODUCTION

42 The seasonal heat flux generates strong seasonal variations in seawater
43 temperature in the Argentine continental shelf (Rivas 2010). In Nuevo Gulf (~ 42 °S,
44 NG in Fig. 1*a.*) the average annual surface heat flux is positive and there is no input
45 from river run-off into the gulf. The heat balance is closed with the advection of cold
46 water from the adjacent continental shelf.

47 Horizontal heat flux is usually an important factor in determining the steady
48 state heat balance, but it has little influence on the seasonal signal (Rivas 1994).
49 Assuming that surface heat flux and temperature can be parameterized with a stationary
50 signal plus an annual harmonic (Rivas and Beier 1990), the harmonics of temperature
51 and heat flux are directly proportional (eq. 1):

52 $$T_1 = \frac{Q_1}{\rho\, C_p\, d\, \omega} \qquad (1.)$$

53 Where T_1 is the annual harmonic amplitude of the seawater temperature; Q_1 is
54 the annual harmonic amplitude of surface heat flux ; ρ is seawater density (~1025
55 Kg/m^3); C_p is the seawater heat capacity (~ 3990 J/kg °C); d (m) is depth and ω is the
56 annual frequency ($2\pi/365$ days).

57 This simple equation shows a hyperbolic growth of the thermal harmonic
58 amplitude as depth decreases (onshore), unless it is limited by a horizontal heat flow. In
59 the present work, we analyze the surface heat flux and time series of water temperature
60 and tide, in order to elucidate the advective mechanisms that modulate the temperature
61 cycle on a seasonal time scale (months) and on shorter time scales (days to weeks)
62 across the shallow nearshore waters of NG (Fig. 1*a.*).

Unlike temperature, there are no systematic measurements of salinity in the area. The available observations indicate that fluctuations are below 0.05 psu. According to estimates of Rivas and Ripa (1989), the influence of salinity gradients in the generation of baroclinic and barotropic flows may be neglected. We suppose that circulation is governed by tide, wind and vertical temperature gradients.

2. DATA AND METHODOLOGY

This study was conducted in an eastward-facing bay (Nueva Bay, NB) located on the west coast of NG, a relatively small embayment on the Argentine continental shelf (Southwestern Atlantic) (Fig. 1). The NG is an elliptical basin with a surface of 2440 km^2 and a maximum depth of 184 m that connects with the continental shelf through a mouth 17 km wide (Mouzo et al. 1978). Dominant tides are semidiurnal with amplitudes of 1.83 m during the neap cycle and 5.73 m during the spring cycle (Tide Tables, (Servicio de Hidrografía Naval 2015). The NB is characterized by strong and persistent westerlies, which are driven by the two anticyclones located in the Atlantic and the Pacific oceans, and a low-pressure belt located around 60° S (Paruelo et al. 1998).

Water temperature was measured at four sites over a cross-shore transect along Luis Piedrabuena Pier (Puerto Madryn, Fig. 1a.) using Onset® Hobo U22-001 water temperature loggers (resolution of 0.02 and accuracy of 0.2 °C between 0 °C and 50 °C). At the first site (A), located ~50 m from the low-tide shoreline and at a mean depth of 3 m, one logger was installed 50 cm above the bottom. Two data loggers were installed at each of the remaining sites (B-D), one ~ 50 cm above the bottom and the other one ~ 50 cm below the surface. Site B was located ~ 500 m from the low-tide shoreline and at a mean depth of ~ 14 m. At this site, three additional thermometers

were installed evenly distributed between surface and bottom. Sites C and D were located ~ 1600/2600 m from the low-tide shoreline and at mean depths of ~29/38 m, respectively (Fig. 1b.). All data loggers were set to record temperatures simultaneously every 10 minutes. Subsequently, those measurements were averaged hourly and the resulting values were used for analysis, smoothing out very high frequency fluctuations. Additionally, hourly anomalies were calculated in order to analyze diurnal and semidiurnal variability. They were computed as the difference between each hourly data and the 24-hour running mean centered on the corresponding datum (eq. 2).

$$AT(t_i) = T(t_i) - \frac{1}{24}\sum_{j=i-11}^{j=i+12} T(t_j) \qquad (2.)$$

Where $AT(t_i)$ is the hourly anomaly at time t_i and $T(t_j)$ is temperature at time t_j.

There are observations from several years available for site B, but only those corresponding to the warm seasons are available for sites C and D (Fig. 1c.). Hourly predictions of tidal level in Puerto Madryn were obtained from the WXTide software Version 4.7, available at http://www.wxtide32.com/. Surface heat flux (sF) between sea and atmosphere was obtained from the NCEP reanalysis (Kalnay et al. 1996) with a temporal resolution of 6 hours. Data from the NCEP reanalysis were compared with previous climatological estimations for the NG based on local atmospheric measurements (Rivas and Ripa 1989) and were considered representative of local conditions.

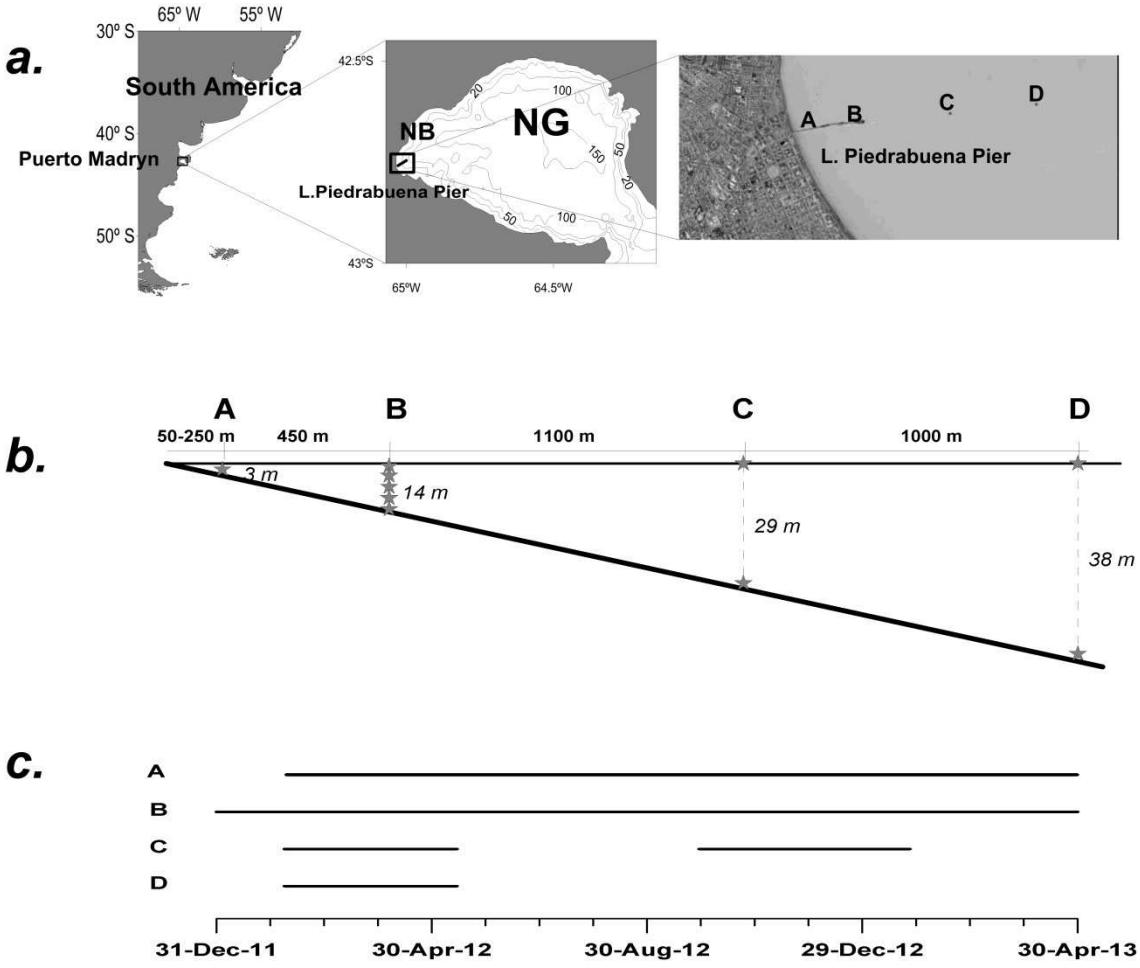

106

107 Figure 1. Geographical location, spatial distribution and temporal extent of the
108 data used. ***a.*** Study area and position of the observation sites at Luis Piedrabuena Pier.
109 Bathymetric contours of Nuevo Gulf (NG) and Nueva Bay (NB) in meters. ***b***. Schematic
110 representation of the relative position of data loggers (gray stars) along the cross-shore
111 transect. ***c.*** Time periods with temperature records for each site.

112

113 3. ANALYSIS AND INTERPRETATION

114 3.1 Seasonal scale

Temperature records in the study area ($d \leq\sim$ 40 m) suggest that seasonal fluctuations were lower than expected considering only sF (seasonal amplitude $Q_1 \sim 200$ W/m^2 according to NCEP reanalysis, see Fig. 2). The time-series show seasonal signal amplitudes of approximately 7°C nearshore ($d<$ 14 m and more than 1 year of records), in agreement with Dellatorre et al. (2012). Maximum and minimum temperatures recorded (~22°C and 8°C respectively) were not as extreme as expected from the integrated sF during the warm (spring-summer) and cold (autumn-winter) seasons, respectively (Fig. 2). Consequently, it is necessary to consider the horizontal heat flux in order to explain the observed seasonal fluctuations, which were smaller than expected.

Assuming that the sF throughout the study area is homogeneous, equation (1.) indicates that horizontal advection should be more intense nearshore. Indeed, this advection should balance the net annual flux and also avoid the excessive temperature increment as d tends to zero. Horizontal advection can be cross-shore or along-shore. However, the data loggers used in this study only allow the evaluation of the heat flux normal to the shore. Recent observations near the study area suggest that along-shore temperature variability is approximately one order of magnitude lower than cross-shore variability (unpublished data).

During the cold season, when sF is from the sea to the atmosphere ($sF< 0$), vertical convection makes the water column homogeneous. Also, this convection is forced at the bottom by the tides and at the surface by the wind. On time scales from weeks to months, the observed vertically averaged temperature should increase offshore. In this case, the advection of offshore warmer water to the nearshore colder area would partly compensate the intense cooling of this shallow area. During the warm

season, when sF is from the atmosphere to the sea (sF> 0), vertical homogeneity only occurs at small depths where wind and/or tide forcing exceed the buoyancy generated by the sF and get to mix the stratified water column. Assuming that this occurs at sites A and B (d<14 m), the cooling/warming attenuation nearshore during warm/cold seasons, respectively, is guaranteed by the sign of the sF and of temperature differences between both sites (T_A-T_B) (Fig. 2).

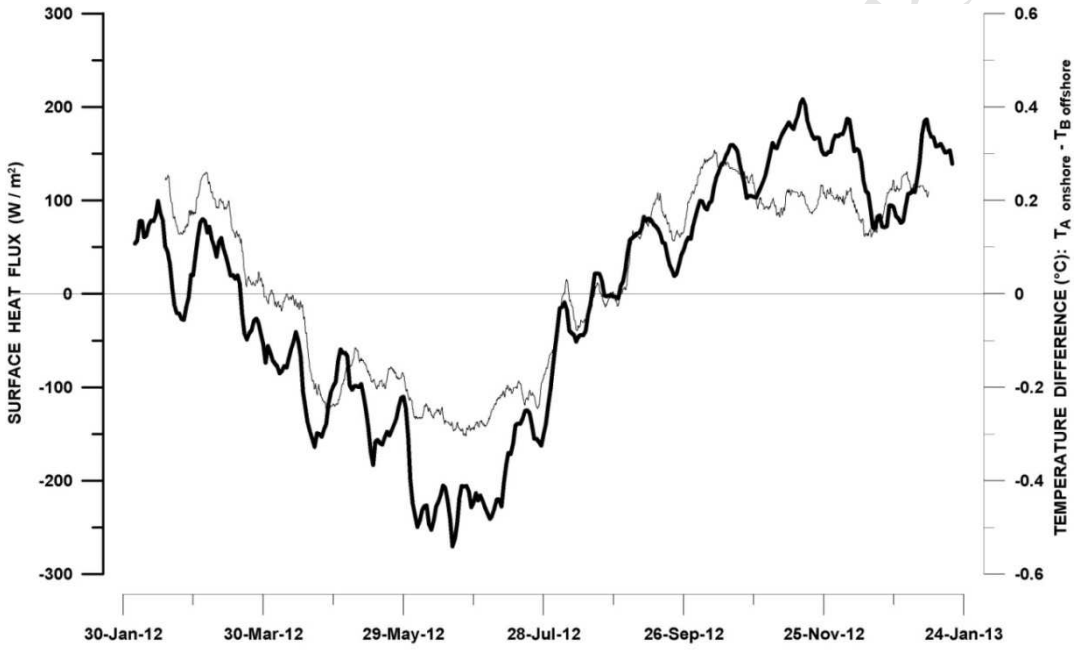

Figure 2. Annual cycle of vertical-averaged temperature difference between sites A (~50 m from shoreline) and B (~500 m from shoreline) (thin line), and surface heat flux (thick line). It is noteworthy that in the warm (cold) season when the heat flow is from the atmosphere (sea) to the sea (atmosphere), the onshore (offshore) temperature is greater, therefore, cross-shore advection attenuates the atmospheric forcing.

Nearshore shallow areas were intensely warmed (cooled) when sF was positive (negative). The differential warming/cooling was self-regulated by means of horizontal heat advection from adjacent deeper regions. Data obtained during summer of 2012 at

153 the moorings where some stratification occurred (site B, d = 14 m, with a difference
154 between surface and bottom temperatures below 1.3°C; site C, d = 29 m with a
155 difference between surface and bottom temperatures below 2.5°C; and at the deepest
156 site D, d = 38 m with a difference between surface and bottom temperatures not greater
157 than 3°C) showed an increase in surface temperature and a decrease in bottom
158 temperature moving away from the coast (see Fig. 3). This temperature distribution is
159 consistent with a simple circulation pattern: cold water from the bottom layer flows
160 towards the coast, upwells and homogenizes the water column in the shallow area, then
161 returns through the surface, and warms by effect of sF as it leaves the coast. This model
162 is similar to the one of Fewings and Lentz (2011) for the North Atlantic. A feedback
163 occurs between vertical and horizontal heat fluxes. A higher surface heat flux generates
164 greater stratification and therefore the horizontal heat flow is bigger because it is
165 directly proportional to the temperature difference between the onshore and offshore
166 waters (bottom and surface flows, respectively).

167

168

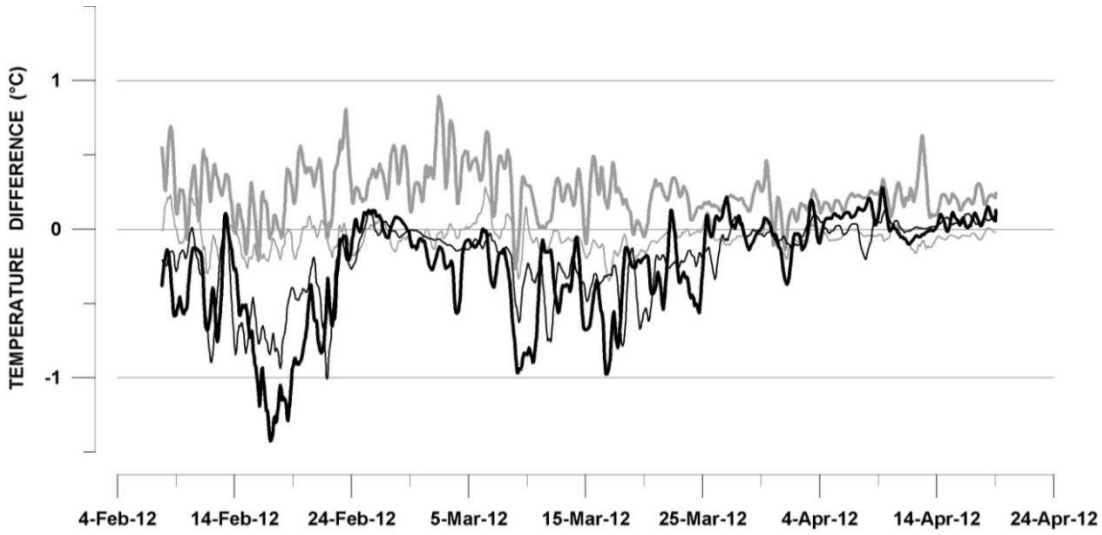

169 Figure 3: Temperature differences between offshore and onshore sites at the
170 bottom (black lines) and at the surface (gray lines). Heavy lines represent temperature
171 differences between site C (~1500 m from the shoreline) and site B (~500 m from the
172 shoreline). Thin lines represent temperature differences between site D (~2500 m from
173 the shoreline) and site C (~1500 m from the shoreline). The data show that bottom
174 (surface) temperature increases onshore (offshore).

175

176 3.2 Diurnal scale

177 At very shallow areas, where tidal amplitude is important relative to the order of
178 magnitude of the average depth (sites A and B), and assuming vertical homogeneity
179 (appropriate in a shallow region with intense winds and tides), the change in heat
180 content of the water column may be expressed as:

181 $$F = \rho C_p \partial_t (d\,T) = \rho C_p (\partial_t d\,T + d\,\partial_t T) \qquad (3.)$$

Where F is total heat flux (vertical and horizontal); ρ is density; C_p is the specific heat capacity of seawater; d is depth (m) and T is the mean vertical temperature (°C).

When considering a change in heat content, it is necessary to consider depth variations of the water column, given that tidal height is important.

Consequently, when F is positive during flood tide ($\partial_t d > 0$), the water column can be heated ($\partial_t T > 0$) or cooled ($\partial_t T < 0$), but during ebb tide ($\partial_t d < 0$), the water column is only warmed. Inversely, when F is negative, the water column during flood tide is only cooled, but during ebb tide it may be warmed or cooled. Furthermore, if the surface flow is positive (negative), the shallow coastal area is warmed (cooled) more efficiently than the surrounding deeper area. That is because the same energy flux per surface area affects a smaller volume of water. During flood and ebb tides, advection occurs onshore and offshore respectively. Offshore advection during ebb tide tends to increase the effect of sF, while onshore advection during flood tide tends to weaken the effect of sF.

There are two ambiguous situations (positive F and flood tide; negative F and ebb tide) in which temperature can increase or decrease, regardless of the direction of the total heat flux. In summer during daylight hours, (sF> 0), the water column at the shallowest site (A) tends to be warmer than in the deeper regions (Eq. 1.). Flood tide (onshore water advection) often causes the cooling of the water column, despite the positive heat flux (see Fig. 4). It is worth mentioning that in this situation, the absolute horizontal heat flux is not necessarily higher than the sF if depth increases rapidly during flood tide (Eq. 3.). Also, during night ebb tides when sF is negative, the horizontal flux should also be negative, advecting nearshore (shallower) colder water. This enhances the effect of negative sF and reduces the possibility of occurrence of

206 unexpected warming during negative sF. These theoretical ideas are supported by data
207 from the shallowest site (A). Summer daily temperature anomalies showed maximum
208 values during daylight hours and at low tide (Fig. 4). During flood tide, the temperature
209 began to decrease although sF was still positive. This was because the product of
210 temperature and depth increment ($T\partial_t d$) during flood tide overcomes the net heat flux.
211 Consequently, the imbalance in Eq. 3 is compensated by a temperature drop. Summer
212 maximum anomaly and temperature at A and surface temperature at B showed a clear
213 daily frequency (Fig. 4), coincident with low tide during daylight. In summer, at night
214 and with low tides, negative sF do not generate significant temperature drops (Fig. 4).
215 Daily surface temperature fluctuations at B were much weaker than at A (Fig. 4). This
216 can be explained by the weaker relative effect of tidal amplitude at a deeper site.

217

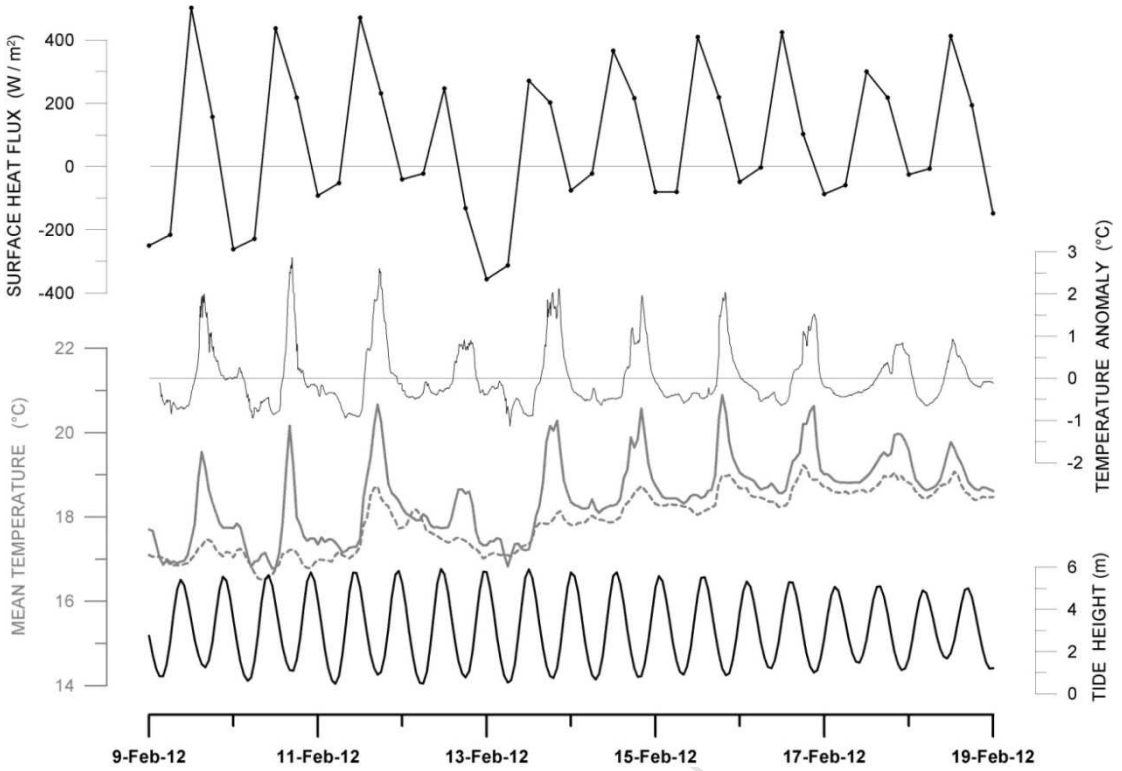

218

219 Figure 4: Surface heat flux (black line with dots every 6 hours, top), daily
220 temperature anomaly in A (~50 m from shoreline, black thin line), temperature in A
221 (thick gray line), surface temperature in B (~500 m from shoreline, dotted gray line) and
222 tidal height (black line, bottom). In summer, temperature and temperature anomaly at
223 station A showed a clear diurnal frequency coincident with daylight and low tide.

224

225 During early autumn (April 2012), absolute values of sF were similar between
226 day (positive) and night (negative) (Fig. 5), and daily surface heat flux tended to zero.
227 At low tide, temperature and temperature anomaly reached maximum (minimum)
228 values according to the sign of sF during the prior hours (Fig. 5). During high tide the
229 effect of sF was minimized and the anomalies were near zero.

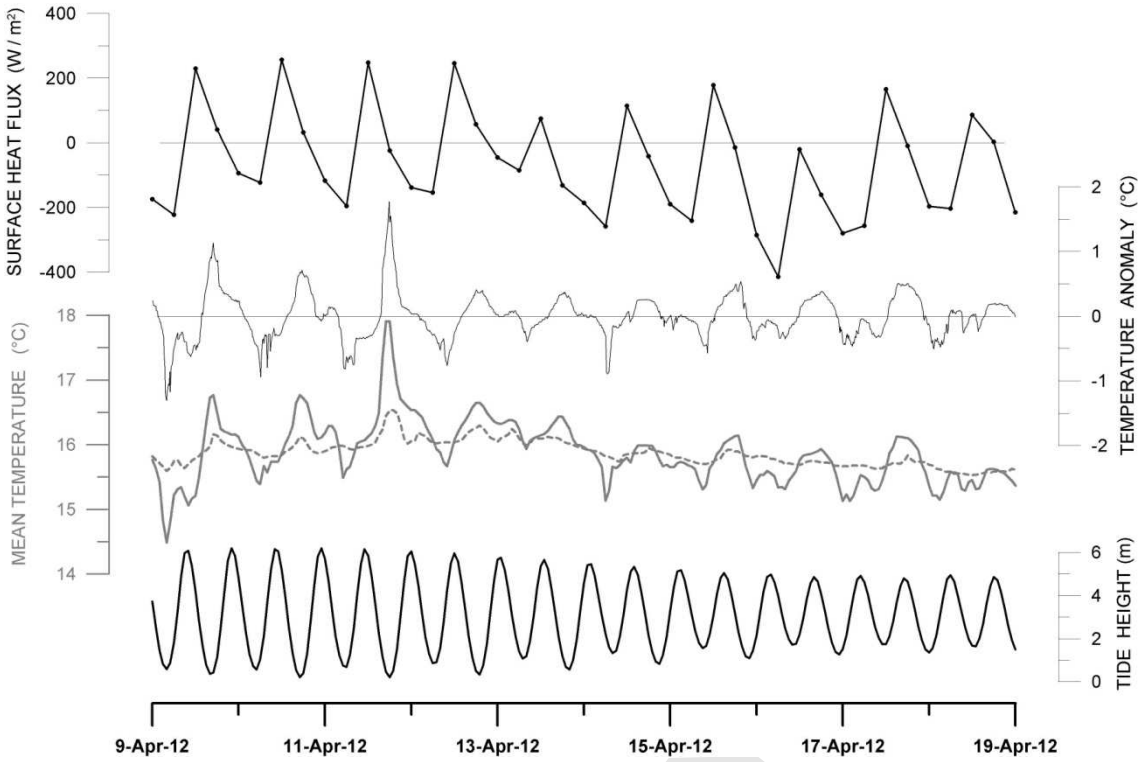

230

231 Figure 5: Surface heat flux (black line with dots every 6 hours, top), daily
232 temperature anomaly in A (~50 m from the shoreline, black thin line), temperature in A
233 (thick gray line), surface temperature in B (~500 m from the shoreline, dotted gray line)
234 and tidal height (black line, bottom). In autumn, temperature and temperature anomaly
235 reach extreme values at low tide. During high tide the effect of sF is minimized and the
236 anomalies are near zero.

237 During periods with daily sF near zero (between 9 and 12 April, Fig. 5),
238 temperature anomalies showed maximum and minimum peaks coincident with low tides
239 in daytime and nighttime, respectively. This demonstrates the amplifier effect of tidal
240 height on sF, during both day and night. It is worth mentioning that tidal amplitudes
241 were the greatest during these days (~6 m) (Fig. 5).

242 On the other hand, when the net sF was negative during both day and night (late
243 autumn and winter), temperature anomaly at A showed a semidiurnal frequency at low

244 tide, whether it was day or night (Fig. 6). However, on days with short periods of
245 positive sF during autumn and winter, temperature at A increased slightly during the day
246 at low tide, and the anomaly oscillated with a diurnal frequency (24-29 May, Fig. 6).

247

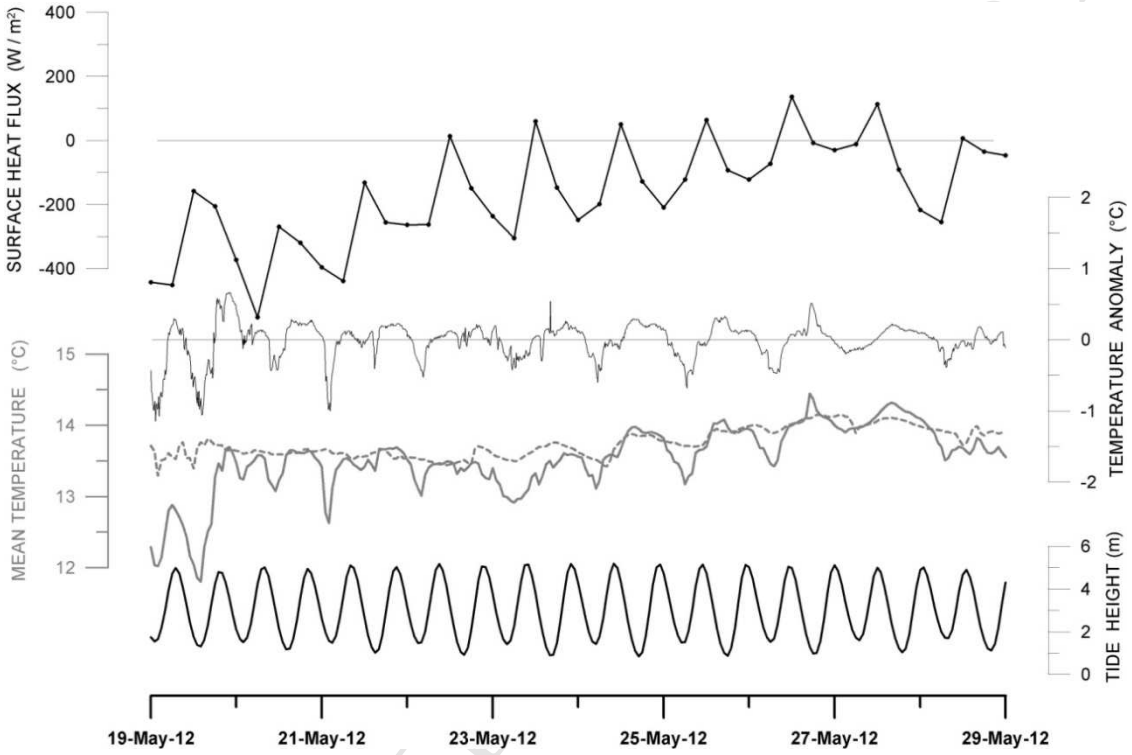

248

249 Figure 6: Surface heat flux (black line with dots every 6 hours, top), daily
250 temperature anomaly in A (~50 m from the shoreline, black thin line), temperature in A
251 (thick gray line), surface temperature in B (~500 m from the shoreline, dotted gray line)
252 and tidal height (black line, bottom). When the surface flux sign is constant (from 19 to
253 22 May-12) the temperature oscillates with a semidiurnal frequency and extreme values
254 are achieved at low tide.

255

Data time-series suggest that ebb tide accentuates the effects of the surface heat flux, given that minimum temperatures were reached when the tide was at its minimum. When tide was rising, surface effects were minimized; the rise in temperature could have been caused by horizontal advection, even when surface heat flux was negative.

4. SUMMARY

In coastal areas surface heat flux was not enough to explain the observed temperature values. Therefore, the effect of heat advection as a temperature regulating mechanism must be considered. Dever and Lentz (1994), Lentz and Chapman (1989), and Lentz (1987) found that variations in the heat balance off the California coast was dominated by a cross-shelf heat flux. On the East Coast of North America during a strong stratified period between May and August, Austin (1999) also showed that the cross-shelf heat flux dominates variations in heat content.

In winter and in those shallow areas where vertical stratification was weak or absent, temperature gradients in the cross-shelf direction indicated that horizontal advection prevented a disproportionate increase in temperature ranges on a seasonal scale. In deeper areas ($d \geq 14$ m) where the water column was stratified during summer, we hypothesize that a cross-shore coastal circulation was generated on a monthly time scale (i.e. independent of wind). Similar to the mechanism described by Fewings and Lentz (2011), the colder flow at the bottom warmed as it moved towards the coast. The water column was homogeneous in the shallower region. A surface flow then moved offshore while its temperature rose as it moved away from the coast (Fig. 7).

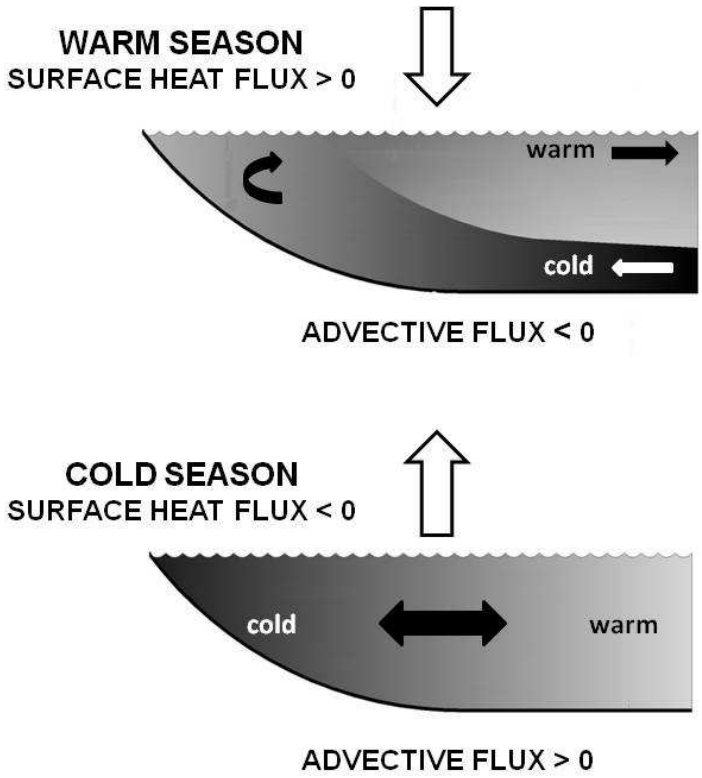

279

280 Figure 7. Schematic representation of the heat balance at a seasonal scale. In
281 winter (cold season), the water column is homogeneous, the net surface heat flux cools
282 shallow waters more efficiently and the cross-shelf flux warms them and compensates
283 for the intense cooling of this area. In summer (warm season) a steady upwelling
284 circulation is established, surface flux controls the temperature difference between
285 surface and bottom and the cross-shelf flux is proportional to this difference.

286

287 In very shallow waters and on an hourly scale, the horizontal advection
288 associated with the rising tide attenuates the atmospheric flux while the falling tide

289 tends to accentuate its influence. This creates diurnal and semidiurnal temperature
290 variations which are basically regulated by tidal height (Fig. 8).

291

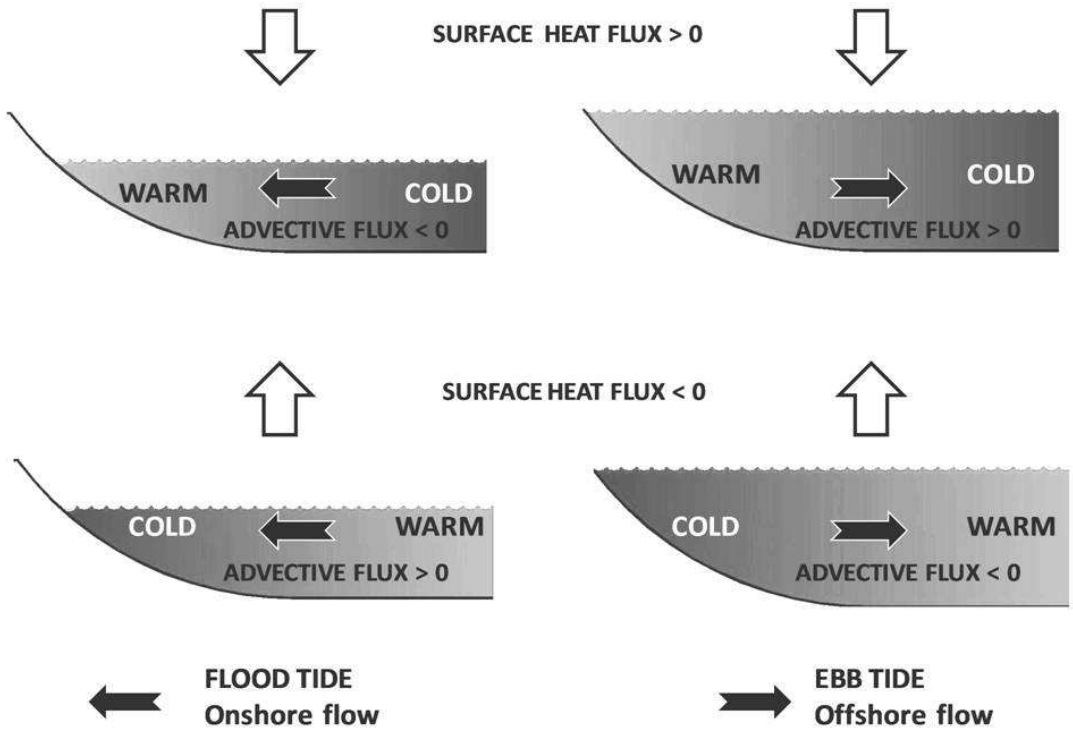

292

293 Figure 8. Schematic representation of the heat balance on an hourly scale. The
294 shallower coastal area is warmed (cooled) more efficiently than the outer area when the
295 surface heat flux is positive (negative). Consistent with flood (left) or ebb tide (right)
296 the horizontal heat flow changes direction, accentuating or attenuating the effect of the
297 atmospheric flow.

298

299 When the coastal region is deep and tide only cause a relatively small change in
300 the mean depth, factors such as wind, especially the sea breeze, begin to play an
301 important role in the variations of coastal water temperature (Dellatorre et al. 2012).

302 At macrotidal coastal sites (with tidal amplitudes of around 4 m, similar to the
303 mean depth), the effective depth can change significantly in just hours, and according to
304 the heat conservation equation (Eq. 3.), this may result in temperature variations in a
305 direction opposite to that suggested by the total heat flow (atmospheric flux and
306 horizontal advection).

307

ACKNOWLEDGMENTS

This work was founded by CONICET (PIP112-200801-03105 and PIP112-201101-01143), and by ANPCyT (PICT 2013-1295). We greatly acknowledge N. Glembocki for english corrections. We wish to acknowledge the authorities of the Harbour Administration of Puerto Madryn, the Nautical staff and Climatology Laboratory of CENPAT.

REFERENCES

Austin JA (1999) The role of the alongshore wind stress in the heat budget of the North Carolina inner shelf. Journal of Geophysical Research 104 (C8): 18187–18203

Dellatorre FG, Pisoni JP, Baron PJ, Rivas AL (2012) Tide and wind forced near-shore dynamics in Nuevo Gulf (Northern Patagonia, Argentina): potential implications for cross-shore transport. Journal of Marine Systems 96-97: 82-89

Dever EP, Lentz SJ (1994) Heat and salt balances over the northern California shelf in winter and spring. Journal of Geophysical Research 99 (C8): 16001–16017

Fewings MR, Lentz SJ (2011) Summertime cooling of the shallow continental shelf. Journal of Geophysical Research 116 (C07015): 2156-2202

Kalnay E, Kanamitsu M, Kistler R, Collins W, Deaven D, Gandin L, Iredell M, Saha S, White G, Woollen J, Zhu Y, Leetmaa A, Reynolds R, Chelliah M, Ebisuzaki W, Higgins W, Janowiak J, Mo KC, Ropelewski C, Wang J, Jenne R, Joseph D (1996) The NCEP/NCAR 40-Year Reanalysis Project. Bulletin of the American Meteorological Society 77 (3): 437–471

Lentz SJ (1987) A heat budget for the northern California shelf during CODE 2. Journal of Geophysical Research 92 (C13): 14491–14509

Lentz SJ, Chapman DC (1989) Seasonal difference in the current and temperature variability over the northern California shelf during the Coastal Ocean Dynamics Experiment. Journal of Geophysical Research 94 (C9): 12571-12592

Mouzo FH, Garza ML, Izquierdo JF, Zibecchi RO (1978) Rasgos de la geología submarina del Golfo Nuevo (Chubut). Acta Oceanográfica Argentina 2: 69-91

Paruelo JM, Beltrán A, Jobbagy E, Sala OE, Golluscio RA (1998) The climate of Patagonia: general patterns and control on biotic processes. Ecología Austral 8: 85-101

Rivas AL (1994) Spatial variation of the annual cycle of temperature in the Patagonian shelf between 40° and 50° of south latitude. Continental Shelf Research 14 (13): 1539-1554

Rivas AL (2010) Spatial and temporal variability of satellite-derived sea surface temperature in the southwestern Atlantic Ocean. Continental Shelf Research 30 (7): 752-760

Rivas AL, Beier EJ (1990) Temperature and salinity fields in the northpatagonic gulfs. Oceanologica Acta 13: 15-20

Rivas AL, Ripa P (1989) Variación estacional de la estructura termohalina del golfo Nuevo. Geofísica Internacional 28 (1): 3-24

Servicio de Hidrografía Naval (2015) Tide Tables. http://www.hidro.gov.ar/oceanografia/tmareas/form_tmareas.asp. Accessed March 30, 2015